

Hadronic properties of the $S_{11}(1535)$ studied by electroproduction off the deuteron

Leonid Frankfurt*

School of Physics and Astronomy, Tel Aviv University, Tel Aviv 69978, Israel

Mikkel Johnson

Los Alamos National Laboratory, Los Alamos, New Mexico 87545, USA

Misak Sargsian^{† ‡} and Wolfram Weise

Physik Department, Technische Universität München, D-85747 Garching, Germany

Mark Strikman[§]

Physics Department, Pennsylvania State University, University Park, PA 16802, USA

(November 17, 2018)

Abstract

Properties of excited baryonic states are investigated in the context of electroproduction of baryon resonances off the deuteron. In particular, the hadronic radii and the compositeness of baryon resonances are studied for kinematic situations in which their hadronic reinteraction is the dominant contribution. Specifically, we study the reaction $d(e, e' S_{11})N$ at $Q^2 \geq 1 \text{ GeV}^2$ for kinematics in which the produced hadronic state reinteracts predominantly with the spectator nucleon. A comparison of constituent quark model and effective chiral Lagrangian calculations of the S_{11} shows substantial sensitivity to the structure of the produced resonance.

*St.Petersburg Nuclear Physics Institute, Gatchina, Russia

†Yerevan Physics Institute, Yerevan, Armenia

‡after 1-May-1998 at University of Washington, Seattle, WA, USA

§St.Petersburg Nuclear Physics Institute, Gatchina, Russia

I. INTRODUCTION

Characterizing the structure of hadrons in the nonperturbative region of QCD is a fundamental issue for understanding nuclear dynamics. One of the key windows for studies of low-energy QCD is the investigation of baryonic resonance properties. Both hadronic and electromagnetic interactions off a free nucleon with excitation of a particular resonance state have been used to carry out such a investigations (for a recent review of this subject see Refs. [1,2]).

In this paper, we address the problem of the investigation of baryonic resonances by studying their electroproduction from a deuteron i.e. $d(e, e'R)N$. Emphasis is to be given to kinematics in which the dominant contribution arises when a resonance produced on one of the nucleons (either the neutron or the proton) undergoes a soft elastic rescattering off the other (spectator or recoil) nucleon. As we will argue, such experiments then offer the possibility of determining the specific properties of the baryonic resonance that are not possible to ascertain by studying production off a single nucleon.

One such property is the hadronic radius of the resonance, a quantity that is crucial for understanding the dynamics governing its composite hadronic structure. Indeed, in a quantum mechanical potential picture, the *virial theorem* shows that the averaged Hamiltonian (H) of the system is determined by the potential (V) and its gradient ($\vec{\nabla}V$):

$$\langle \psi | H | \psi \rangle = \langle \psi | V | \psi \rangle + \frac{1}{2} \langle \psi | \vec{r} \cdot \vec{\nabla} V(r) | \psi \rangle. \quad (1)$$

From the above equation, e.g. for the Coulomb potential, one obtains $\langle \frac{1}{r} \rangle = \frac{mZ\alpha}{n^2}$, while for harmonic oscillator potential $\langle r^2 \rangle = \frac{(n+\frac{1}{2})}{mw}$. Here n is the principal quantum number. The above examples illustrate that at least for certain types of potentials, excited states have larger radii than ground states. Moreover, knowing the dependence of the radius on the quantum number of the excitation may allow one to determine the interaction.

The issue of the radius of excited hadronic states also crucial for understanding the duality between the quark-gluon and the hadronic descriptions of the strongly interacting system. Indeed, several experimental observations, such as the A dependence of the coherent photoproduction of J/Ψ mesons from nuclei [3], the energy dependence of the diffractive electroproduction of vector mesons with coherent nuclear recoil [4,5], and coherent pion diffraction into two jets [6], indicate a reasonably broad distribution (fluctuation) of the interaction cross section for color singlet objects (possibly indicating color transparency and color opacity phenomena; see Ref. [7] for details). To saturate the sum rule for the distribution of the cross section, one should assume a significant probability for the cross section to be larger than average. One of the ideas for realizing such large cross sections is to adopt larger sizes for hadronic resonances.

Another property of interest is the compositeness of the produced state - whether it be a single baryonic resonance or the superposition of multichannel *meson* - *baryon* components with a strong attraction that makes a resonance-like quasi-bound system. From the point of view of the production of excited hadronic states from an isolated nucleon, it is difficult to identify a signature to distinguish a single baryonic resonance from a multichannel *meson* - *baryon* system when some of the channels contain a strong attraction, thus imitating the resonance-like mass distribution.

However if the nucleon is inside the nucleus, then the resonance or multichannel nature of the excited hadronic state would provide a qualitatively different picture for hadronic reinteractions with the spectator nucleons of the nucleus. This is the main idea which we are going to exploit in studying properties of the excited hadronic states.

Specifically we will consider the electroproduction of the $S_{11}(1535)$ resonance in the $d(e, e'S_{11})n$ reaction, where the neutron will be detected as a spectator. The choice of the $S_{11}(1535)$ is suggested by two important characteristics of this resonance: first, the $S_{11}(1535)$ has a large cross section for the electromagnetic NN^* transition and a weak $NN \rightarrow NN^*$ transition; and, second, the $S_{11}(1535)$ has a large $N\eta$ branching ratio (up to 55%), which makes it experimentally easily detectable. To gain a feeling for the sensitivity of the $d(e, e'S_{11})n$ reaction to the hadronic structure of the $S_{11}(1535)$, we will obtain predictions from two basically different approaches. In the first case, the $S_{11}(1535)$ is represented as an excited baryonic state whose structure is described in terms of quark constituents. For the second, the $S_{11}(1535)$ represents a strongly enhanced structure in the amplitude of a four-channel meson-baryon system with total isospin $\frac{1}{2}$.

Within the constituent quark model (CQM) classification, the $S_{11}(1535)$ belongs to the $[70, 1^-]_1$ supermultiplet and represents an $L = 1$ radial excitation of the nucleon (see e.g. Ref. [1]). In a typical constituent-quark model with a harmonic oscillator ansatz for the interacting potential (e.g. [8,9]), the larger radial extension of the $L = 1$ wave function means that the distribution of quarks in the S_{11} should be more spread out than the one for the nucleon.

A second approach is based on the framework developed in Refs. [10–12], where effective potentials for the interaction of pseudoscalar Goldstone bosons (π , K , η) with octet baryons (N , Λ , Σ , Ξ) have been derived from an $SU(3)$ effective chiral Lagrangian (ECL), with QCD chiral symmetry breaking due to non-vanishing up, down and strange quark masses. While solving a coupled-channel Schrödinger equation with the above mentioned potentials for the four-channel system of πN , ηN , $K\Lambda$, and $K\Sigma$ states with total isospin $\frac{1}{2}$, it was found in Refs. [10,11] that the properties of the $S_{11}(1535)$ can be well-described as an S -wave superposition of these four states. Moreover, the strong S -wave attractive interaction of the $K\Sigma$ system can build a quasi-bound state with the characteristics of the $S_{11}(1535)$. This approach naturally solves the problem of the large branching ratio of $S_{11}(1535)$ decay to ηN , showing it to be a consequence of the strong coupling of the πN and ηN channels to the $K\Sigma$ channel [10–12]. The fact that the properties of the $S_{11}(1535)$ do hardly change in nuclei, as observed in the nuclear photoproduction of η meson [33], is consistent with the ECL picture.

The CQM and ECL approaches described above reproduce fairly well the main features of the $S_{11}(1535)$ resonance, but it seems that reactions involving only one nucleon can not distinguish between these two models. However, scattering on the deuteron provides the possibility of a different reaction mechanism, namely the soft rescattering of the S_{11} on the spectator nucleon. Thus, if one selects kinematics in which the dominant contribution to $d(e, e'S_{11})n$ arises when the resonance produced from the proton rescatters on the spectator neutron, one will substantially increase the sensitivity of the reaction to the hadronic properties of the S_{11} and possibly provide a means to distinguish the two approaches.

As an independent development, in Refs. [13] the quasielastic $d(e, e'N)N$ reaction was calculated within the generalized eikonal approximation (GEA). It was demonstrated that

one can indeed identify specific kinematics for which the dominant contribution comes from the rescattering of the knocked-out nucleon on the spectator nucleon. Such a contribution is provided at large transverse momenta of the spectator nucleon with respect of the momenta of virtual photon. Calculations in Ref. [13] demonstrate that starting at $Q^2 \geq 1 \text{ GeV}^2$ the eikonal approximation is well justified: in its low-energy limit, with a transferred energy of 0.5 GeV , the GEA agrees (within 5-10%) with the results of the calculations of Ref. [14]. In Ref. [14], the eikonal approximation was not used, but the contributions of a large number of partial-waves (up to eight) were summed.

In this paper, we will incorporate the GEA method into the CQM and ECL frameworks for describing the S_{11} and calculate the $d(e, e'S_{11})n$ reaction at $Q^2 \geq 1 \text{ GeV}^2$. The results of the CQM will demonstrate that for kinematics where the rescattering contribution to the $d(e, e'S_{11})n$ reaction is dominant there is a substantial sensitivity to the hadronic size of the final state produced. Significantly different predictions are made within the CQM as compared to the ECL approximation.

We first (in Section II) set up the kinematics and calculational procedure for $d(e, e'S_{11})n$ within the generalized eikonal approximation. The structure of $S_{11}(1535)$ will then be incorporated using the constituent quark model and the chiral dynamics approach. In Section III, the results of our numerical estimates will be discussed. In Section IV, we will discuss a class of resonances that may be investigated in a similar way. Finally, in Section V we will summarize the paper.

II. SETTING UP THE KINEMATICS AND CROSS SECTION

A. Kinematics

As a first step, to establish the relevant kinematics, we consider the special situation for which the $S_{11}(1535)$ resonance is produced off a nucleon with small Fermi momentum. One way to fix the kinematics corresponding to the production of the S_{11} resonance off a quasifree nucleon (almost at rest) is to choose $x \equiv \frac{Q^2}{2mq_0}$ to be

$$x = 1 - \frac{m_R^2 - m^2}{Q^2 + m_R^2 - m^2}. \quad (2)$$

Here q_0 and $-Q^2$ are the energy and four-momentum squared of the virtual photon, and m and m_R are the masses of the nucleon and the S_{11} resonance, respectively. We define also the mass W of the produced hadronic state as:

$$W^2 = (q + m_d - p_s)^2, \quad (3)$$

where $q \equiv (q_0, \mathbf{q})$ and $p_s \equiv (E_s, \mathbf{p}_s)$ are the four-momenta of the virtual photon and spectator nucleon respectively.

To ensure that the process occurs off a nucleon with small Fermi momentum, we shall also require that the light-cone momentum of the recoil nucleon (fraction of the deuteron momentum carried by spectator nucleon) be near one [13], i.e.

$$\frac{E_s - p_{sz}}{m} \approx 1. \quad (4)$$

The z axis is defined by the direction of virtual photon \mathbf{q} . Note, however, that we will require that the transverse momentum of the spectator be $p_{st} \lesssim 0.4 \text{ GeV}/c$ to ensure that the dominant contribution arises from the rescattering diagram. Using this restriction on the Fermi momentum, one can also neglect any contribution from the N^* component of the deuteron ground state wave function and end up with the set of diagrams presented in Fig.1.

B. Cross Section of the Reaction

In general, the differential cross section of the $d(e, e'R)n$ reaction, where the momentum of the scattered electron and spectator nucleon are measured in the final state, can be represented as follows:

$$\frac{d^6\sigma}{dE'_e d\Omega_e d^3p_s} = \frac{2\alpha}{Q^4} \frac{E'_e}{E_e} \eta_{\mu\nu} w^{\mu,\nu} \quad (5)$$

where $\alpha = \frac{1}{137}$, the four-momenta of the incoming and scattered electrons are $k_e^\mu = (E_e, \mathbf{k}_e)$ and $k_e^{\mu'} = (E'_e, \mathbf{k}'_e)$ respectively, and $\eta_{\mu\nu} = \frac{1}{2} \text{Tr}(\hat{k}'_e \gamma^\mu \hat{k}_e \gamma^\nu)$ is the leptonic tensor. The hadronic tensor can be expressed through the electromagnetic transition amplitude of the deuteron F^μ as follows:

$$w^{\mu,\nu} = \sum_{s_i} \sum_{s_f} \bar{F}^\mu F^{\nu\dagger}, \quad (6)$$

where we average over the initial and sum over the final spin states. It is convenient to express the cross section in eq.(5) through the four invariant functions σ_T , σ_L , σ_{TT} and σ_{TL} as follows:

$$\frac{d^6\sigma}{dE'_e d\Omega_e d^3p_s} = \frac{\alpha}{2\pi^2} \frac{E'_e K}{Q^2 E_e (1 - \epsilon)} \left\{ \sigma_T + \epsilon \sigma_L - \epsilon \cos(2\phi) \sigma_{TT} + \sqrt{\epsilon(\epsilon + 1)} \cos(\phi) \sigma_{TL} \right\} \quad (7)$$

where $\epsilon = [1 + 2 \tan^2(\frac{\theta_e}{2}) \frac{\mathbf{q}^2}{Q^2}]^{-1}$ and ϕ defines the azimuthal angle between the (k_e, k'_e) and (k_e, p_s) planes. The four invariant structure functions defined as:

$$\begin{aligned} \sigma_T &= \frac{4\pi^2\alpha}{K} \frac{w^{x,x} + w^{y,y}}{2} \\ \sigma_L &= \frac{4\pi^2\alpha}{K} \frac{\mathbf{q}^2}{Q^2} \left[w^{0,0} - 2 \frac{q_0}{\mathbf{q}} w^{0,q} + \left(\frac{q_0}{\mathbf{q}} \right)^2 w^{q,q} \right] \\ \sigma_{TT} &= \frac{4\pi^2\alpha}{K} \frac{w^{x,x} - w^{y,y}}{2} \\ \sigma_{TL} &= \frac{4\pi^2\alpha}{K} \sqrt{\frac{2\mathbf{q}^2}{Q^2}} \left[\frac{q_0}{\mathbf{q}} w^{q,y} - w^{0,y} \right] \end{aligned} \quad (8)$$

Thus, knowledge of the electromagnetic transition amplitude F^μ will allow us to calculate all of the above structure functions and the differential cross section of eq.(7). To proceed,

we express $F^\mu = F_a^\mu + F_b^\mu$. Here, F_a^μ describes a transition amplitude within the impulse approximation when the resonance produced on one nucleon does not experience any further interaction (see Fig.1a), and F_b^μ describes the amplitude where additional rescattering of the electromagnetically produced hadronic system is taking place (see Fig.1b). Next we shall outline the calculation of the F_a^μ and F_b^μ amplitudes.

1. Impulse approximation

The scattering amplitude within the impulse approximation (IA) corresponds to the diagram of Fig.1a, where the S_{11} produced by the electromagnetic interaction does not interact further with spectator nucleon

$$F_a = (2\pi)^{\frac{3}{2}} \psi(p_s) A^\mu(Q^2), \quad (9)$$

where $A^\mu(Q^2)$ is the electromagnetic γNN^* transition amplitude and ψ is the nonrelativistic deuteron wave function normalized as $\int |\psi|^2(p) d^3p = 1$.

2. Rescattering amplitude

We next consider the rescattering amplitude of Fig.1b, where the hadronic system (h) produced in an electromagnetic scattering on one nucleon rescatters off the second spectator nucleon producing the S_{11} in the final state. Suppressing the spin indices, the rescattering amplitude can be represented as follows (see e.g. [13,15]):

$$F_b^\mu = \frac{1}{\sqrt{2m}} \sum_h \int \frac{A_h^\mu(Q^2) \Gamma(p_d, p'_s) f^{hN \rightarrow N^*n}(p_f, p'_s, p_s)}{[(p_d - p'_s)^2 - m^2 + i\epsilon][p_s'^2 - m^2 + i\epsilon][(p_f + p_s - p'_s)^2 - m_h^2 + i\epsilon]} \frac{d^4 p'_s}{i(2\pi)^4}, \quad (10)$$

where, p'_s and p_s are the momenta of the spectator nucleon in the intermediate and final state, respectively, p_f is the momentum of the S_{11} in the final state, $\Gamma(p_d, p'_s)$ is the invariant vertex of the transition $d \rightarrow pn$ into two off-mass shell nucleons, and $f^{hN \rightarrow N^*N}$ are the $hN \rightarrow S_{11}N$ diffractive transition amplitudes. All spin dependences of the target nucleons are included in the vertex factor. Here $\frac{1}{\sqrt{2m}}$ arises from the normalization of the spectator nucleon wave function. Using a non-relativistic description of Fermi motion in the deuteron allows us to evaluate the loop integral by taking the residue over the spectator nucleon energy in the intermediate state, i.e. we can replace $[p_s'^2 - m^2 + i\epsilon]^{-1} d^0 p'_s$ by $-i(2\pi)/2E'_s \approx -i(2\pi)/2m$. This is possible because, in this case, there is only one nearby pole in the lower part of the p'_{s0} complex plane (see for details Refs.([13,15])).

The calculation of the residue in p'_{s0} fixes the time ordering from the left to the right in diagram Fig.1b. We introduce the nonrelativistic deuteron wave function as $\psi(p_d - p'_s) \equiv \frac{\Gamma^{d \rightarrow pn}}{[(p_d - p'_s)^2 - m^2 + i\epsilon] \sqrt{(2\pi)^3 2m}}$ (with $\int |\psi(k)|^2 d^3k = 1$). Performing above integration we obtain

$$\begin{aligned} F_b^\mu &= -\frac{(2\pi)^{\frac{3}{2}}}{2m} \sum_h \int A_h^\mu(Q^2) \psi(p'_s) \frac{f^{hN \rightarrow N^*N}(p_f, p'_s, p_s)}{[(p_f + p_s - p'_s)^2 - m_h^2 + i\epsilon]} \frac{d^3 p'_s}{(2\pi)^3} \\ &= -\frac{(2\pi)^{\frac{3}{2}}}{2} \sum_h \int A_h^\mu(Q^2) \psi(p'_s) \frac{f^{hN \rightarrow N^*N}(p_{st} - p'_{st})}{2m p_{fz} [p'_{sz} - p_{sz} + \Delta + i\epsilon]} \frac{d^3 p'_s}{(2\pi)^3}, \end{aligned} \quad (11)$$

where

$$\Delta = (E_s - m) \frac{E_f}{p_{fz}} - (p_{st} - p'_{st}) \frac{p_{ft}}{p_{fz}} + \frac{W^2 - m_h^2}{2p_{fz}}, \quad (12)$$

where $W = p_f^2$ defined according to eq.(3). In the last part of eq.(11) we used energy-momentum conservation to express the propagator of the hadrons h produced in the intermediate state as:

$$\begin{aligned} & (p_f + p_s - p'_s)^2 - m_h^2 = \\ & 2p_{fz} \left[p'_{sz} - p_{sz} + (E_s - m) \frac{E_f}{p_{fz}} - (p_{st} - p'_{st}) \frac{p_{ft}}{p_{fz}} + \frac{(p_s - p'_s)^2}{2p_{fz}} + \frac{W^2 - m_h^2}{2p_{fz}} \right] \\ & \approx 2p_{fz} [p'_{sz} - p_{sz} + \Delta]. \end{aligned} \quad (13)$$

The fact that the energy transferred in the soft $hN \rightarrow N^*N$ rescattering is small compared to the total energy of the scattered particles allows us to neglect the term $\frac{(p_s - p'_s)^2}{2p_{fz}}$ ($\sim \frac{(\vec{p}_s - \vec{p}'_s)^4}{8m^2 p_{fz}} - \frac{(\vec{p}_s - \vec{p}'_s)^2}{2p_{fz}}$ with $|\vec{p}_s - \vec{p}'_s| \approx 0.2 \text{ GeV}/c$) as compared to the other contributions to Δ .

We keep the term $(E_s - m) \frac{E_f}{p_{fz}}$ because it does not vanish with an increase of the projectile energy at fixed spectator nucleon momentum. The term $(p_{st} - p'_{st}) \frac{p_{ft}}{p_{fz}}$ vanishes for the kinematics being considered, where p_f is nearly parallel to the momentum of virtual photon. The last term proportional to $\frac{m_{N^*}^2 - m_h^2}{2p_{fz}}$ takes into account minimal longitudinal momentum need to be transferred to make a nondiagonal $h - N^*$ transitions. Because this term enters as an effective longitudinal momentum into the argument of the deuteron wave function it suppress the contributions of intermediate states h with masses far from m_{N^*} .

The fact that the soft scattering amplitude depends only weakly on the initial energy helps to simplify eq.(11). It is convenient to redefine the soft scattering amplitude $\frac{f^{hN \rightarrow N^*n}(p_f, p'_s, p_s)}{2p_{fz}m} \approx f^{hN \rightarrow N^*n}(p_s - p'_s)$, where $f^{hN \rightarrow N^*n}$ is now the soft scattering amplitude normalized similarly to the elastic amplitude, which is in turn normalized by the optical theorem $Im f^{hN \rightarrow hN}(k=0) = \sigma_{hN \rightarrow hN}^{tot}$.

Then, introducing the transferred momenta $k = p_s - p'_s$, eq.(11) can be rewritten as

$$F_b^\mu = -\frac{(2\pi)^{\frac{3}{2}}}{2} \sum_h \int \psi_d(p_s - k) A_h^\mu(Q^2) \frac{f^{hN \rightarrow N^*N}(k)}{[-k_z + \Delta + i\epsilon]} \frac{d^3k}{(2\pi)^3}. \quad (14)$$

In eq.(14), the only quantities to be specified are the electromagnetic transition amplitude $A_h^\mu(Q^2)$ and the soft rescattering amplitude $f^{hN \rightarrow N^*N}(p_s - p'_s)$.

In next two sub-sections we will discuss the constituent quark model and the chiral dynamic approach and perform the calculation of the impulse approximation (F_a^μ) and rescattering (F_b^μ) amplitudes in each of them.

C. Predictions within CQM approach

Within the constituent quark model approach, we assume that the intermediate states are either nucleons (N) or an N^* resonance, whose structure is described by the CQM.

Furthermore, we neglect the $NN \rightarrow N^*N$ transition amplitude compared to the amplitude of elastic $N^*N \rightarrow N^*N$ scattering. The relative suppression of the transition amplitude compared to the elastic amplitude is supported by experimental observation in Ref. [16], which gives upper limit of such suppression as $\frac{\sigma_{NN \rightarrow N^*N}}{\sigma_{N^*N \rightarrow N^*N}} \sim \frac{1}{20}$. Another source of suppression is our choice of kinematics in eq.(2). Because this corresponds to the production of an N^* resonance off a quasifree nucleon and $x < 1$, the struck nucleon (N) in the initial state is highly virtual. The resulting phase change in the amplitude is $\exp(i\Delta Ez)$, where according to eq.(12) $\Delta E \approx \frac{m_{N^*}^2 - m^2}{2p_{fz}}$ accounts for the virtuality of the intermediate nucleon. Since this phase will contribute a longitudinal component of momentum into the deuteron wave function, one can estimate the suppression as $\frac{|\psi_D(\Delta E)|}{|\psi_D(p \approx 0)|}$.

One gains a further simplification by neglecting the charge exchange contribution in the soft rescattering amplitude. Neglecting this is justified by the fact that the charge-exchange amplitude is predominantly real due to its pion-exchange nature. Thus, it will interfere mainly with the real part of the diffractive N^*N amplitude, which is $\leq 5\%$ of the total cross section (see discussion in Ref. [13]).

The two approximations mentioned above will allow us to factorize the electromagnetic amplitude in F_b^μ so that we finally obtain:

$$F_b^\mu = -A_{N^*}^\mu(Q^2) \frac{(2\pi)^{\frac{3}{2}}}{2} \int \psi(p_s - k) \frac{f^{N^*N \rightarrow N^*N}(k)}{[-k_z + \Delta + i\epsilon]} \frac{d^3k}{(2\pi)^3}. \quad (15)$$

Here

$$\Delta = (E_s - m) \frac{E_f}{p_{fz}} - (p_{st} - p'_{st}) \frac{p_{ft}}{p_{fz}} + \frac{W^2 - m_{N^*}^2}{2p_{fz}} + i\Gamma m_R / (2p_{fz}), \quad (16)$$

where the term $i\Gamma m_R / (2p_{fz})$ accounts for the mass width of the resonance produced in the intermediate state (see e.g. [21]). The size of this correction decreases with increasing energy, and in the high-energy limit the location of the pole will be again defined by the mass of the propagating resonance.

In eq.(15) $f^{N^*N \rightarrow N^*N}$ is the small angle elastic scattering amplitude, which can be represented in the form (see e.g. Ref. [17]):

$$f_{N^*N \rightarrow N^*N}(t) \approx \sigma_{N^*N}^{tot}(i + \alpha) e^{\frac{b}{2}t}, \quad (17)$$

where $\sigma_{N^*N}^{tot}$ is the total N^*N scattering cross section, b defines the slope factor of the elastic differential cross section, and α accounts for the real part of the amplitude.

To construct the soft amplitude $f^{N^*N \rightarrow N^*N}$ within the CQM framework, the idea is to exploit the fact that in general the small-angle elastic hN scattering depends on the radius of the hadron in a characteristic fashion. In particular, the hadronic radii of the interacting particles are related (see e.g. Refs. [18–20]) to the total scattering cross section σ_{hN}^{tot} as follows,

$$\sigma_{hN}^{tot} = \sigma_{NN}^{tot} \frac{\langle r_h^2 \rangle}{\langle r_N^2 \rangle}, \quad (18)$$

and to the slope parameter b ,

$$b \approx \frac{1}{3} \left(\langle r_h^2 \rangle + \langle r_N^2 \rangle \right), \quad (19)$$

appearing in Eq.(17). It follows from eqs.(17), (18) and (19) that if we implement elastic $S_{11}N$ scattering based on the well established characteristics of the nucleon we can establish the spatial parameters of the S_{11} resonance.

One may now recall that within the CQM, the mean-square radius of a quark orbit, $\langle r^2 \rangle$, scales roughly as $2N + L + 3/2$, where N is the number of radial nodes and L is the orbital angular momentum in the wave function. Thus, the spatial distribution of the quarks is quite sensitive to their orbital excitation within the individual resonances.

To estimate the dependence of the reaction on the size of the hadrons in the CQM, it is first necessary to eliminate the dependence on the center-of-mass coordinate in the hadron wave function. In the zero-order quark shell model of Ref. [8] this wave function is $\Psi = \phi(N_\rho, L_\rho, \rho)\phi(N_\lambda, L_\lambda, \lambda)$, where $\rho^2 = (r_1 - r_2)^2/2$ and $\lambda^2 = (r_1 + r_2 - 2r_3)^2/6$ with r_1 , r_2 , and r_3 being the coordinates of the three constituent quarks. The quantities N_ρ and L_ρ represent the radial and orbital excitation quantum numbers. One then obtains the following relation for the radius of the baryons in terms of the mean-square radii of the two independent harmonic oscillators:

$$\langle r^2 \rangle = [(2N_\lambda + L_\lambda + 3/2) + (2N_\rho + L_\rho + 3/2)]b_{hosc}^2. \quad (20)$$

where b_{hosc}^2 is the slope factor of the Harmonic Oscillator wave function of constituent quark. For the nucleon, $(N, L) = (0, 0)$ for both sets of quantum numbers, and $\langle r_{nucl}^2 \rangle = 3b_{hosc}^2$. For the S_{11} one set of $(N, L) = (0, 0)$ and the other is $(0, 1)$. This gives $\langle r_{s11}^2 \rangle = 4b_{hosc}^2$. Therefore according to eqs.(18,19) one obtains:

$$(\sigma_{hN}^{tot}, b) = \left(\frac{4}{3}\sigma_{NN}^{tot}, \frac{7}{6}b_{NN} \right). \quad (21)$$

The coefficients on the right-hand side may be larger than those given here, since the harmonic oscillator model may overestimate the effect of confinement. For a sufficiently sensitive experiment of the type we propose here, one should be able to determine the extent to which the S_{11} resonance is larger than a nucleon.

D. Predictions within the ECL approach

Within the chiral SU(3) dynamics approach, the S_{11} represents a superposition of $N\pi$, $N\eta$, ΛK , and ΣK states with total isospin $\frac{1}{2}$ [10]. One can therefore describe the intermediate state of Fig. 1b by these four states, which then interact with the spectator nucleon. Such a picture will correspond to the following rescattering amplitude in Eq.(14):

$$F_b^\mu = -\frac{(2\pi)^{\frac{3}{2}}}{2} \sum_i \int \psi(p_s - k) A_i^\mu(Q^2) \frac{f^{iN \rightarrow jN}(k)}{[-k_z + \Delta_{ij} + i\epsilon]} \frac{d^3k}{(2\pi)^3}, \quad (22)$$

where $i, j = (1-4)$ represent the four relevant meson-baryon channels states: $N\pi$, $N\eta$, ΛK , and ΣK , respectively, and A_i^μ are the amplitudes for the corresponding electromagnetic transitions $\gamma N \rightarrow N\pi, N\eta, \Lambda K, \Sigma K$. We take $\sum_i \equiv \sum_i \int \frac{d^3k_i}{(2\pi)^3}$, with the $1/2\sqrt{m_i^2 + p_f^2}$ term

absent because of the normalization used for the rescattering amplitude (see before of the eq.(14)). The quantity Δ_{ij} , which accounts for the longitudinal momentum transfer is:

$$\Delta_{ij} = (E_s - m) \frac{E_f}{p_{fz}} - (p_{st} - p'_{st}) \frac{p_{ft}}{p_{fz}} + \frac{m_i^2 - m_j^2}{2p_{fz}}, \quad (23)$$

where $m_i = (\sqrt{m_M(i) + k_i} + \sqrt{m_B(i) + k_i})^2$ is the off-shell invariant mass of the intermediate system. Accordingly, $m_j \equiv W$ is the mass of the final state hadronic system.

In eq.(22), $f^{iN \rightarrow jN}(q)$ corresponds to the scattering of the initial correlated meson-baryon pair "i" off the spectator nucleon to the final correlated meson-baryon pair in state "j" with the spectator nucleon recoiling. The amplitude of such a scattering can be represented through the transition form-factors $S_{i,j}(q)$ (see e.g. Refs. [22,23]) as follows:

$$f^{iN \rightarrow jN}(k) = f^{MN}(k) S_{i,j}(a_1 \cdot k) + f^{BN}(k) S_{i,j}(-a_2 \cdot k) + \frac{i}{2} \int \frac{d^2 k'_\perp}{(2\pi)^2} f^{MN}(a_1 \cdot k - k') f^{BN}(a_2 \cdot k + k') S_{i,j}(k'_\perp) \quad (24)$$

where $a_1 = \frac{m_B}{m_B + m_M}$ and $a_2 = \frac{m_M}{m_B + m_M}$ (M and B defines the meson and the baryon which belongs to the intermediate "i" state) f^{MN} and f^{BN} are the diffractive amplitudes of the meson-nucleon and baryon-nucleon small angle scattering, defined in the form of eq.(17). The $S_{i,j}(q)$ is the transition structure function of the meson-baryon system:

$$S_{i,j}(k) = \int d^3 r \psi_{k_i}(r) \psi_{k_j}^\dagger(r) e^{-i\vec{k}\vec{r}}, \quad (25)$$

where $\psi_{k_i}(r)$ is meson-baryon wave function for channel i , which can be expressed (see e.g. [24]) as follows

$$\psi_{k_i}(r) = \phi_{k_i}^i + \sum_n \int \frac{d^3 l}{(2\pi)^3} \frac{\phi_{k_n}^n < l | T_{ni} | k_i >}{k_n^2 - l^2 + i\epsilon}. \quad (26)$$

Here, the on-mass shell momentum is defined as $k_n^2 = \frac{[W^2 - (m_B(n) + m_M(n))^2][W^2 - (m_B(n) - m_M(n))^2]}{4W^2}$. In eq.(26) ϕ^i is the plane wave function for state i and T_{ni} is the t-matrix of the $n \rightarrow i$ transition, which represents the solution of the coupled channel Lippmann-Schwinger equation [10,11]. In the calculations, we made the partial wave decomposition of the wave function in eq.(25) using the relation (for any operator A) [25]:

$$< k' | A | k > = 4\pi \sum_l (2l + 1) P_l(k', k) < k' | A_l | k >, \quad (27)$$

retaining only the S -wave ($l = 0$) contribution. Such a restriction is justified by the fact that eq.(24) corresponds to small-angle scattering, where the main contribution comes from momenta $k \leq 200 \text{ MeV}/C$. Since q enters into S_{ij} as $a_{1,2}k$, even smaller momenta are relevant for the rescattering amplitude.

Finally we note that for both the electromagnetic amplitude $A_i^\mu(Q^2)$ and the matrix T_{ni} we use the calculation of the Ref. [11,26].

III. NUMERICAL ESTIMATES

For the numerical results we present in this section, we assume that the quantities measured are the momenta of the final electron and the spectator neutron.

To assess to what extent the hadronic structure of S_{11} is revealed in the rescattering processes, we must first ensure that the rescattering (amplitude F_b^μ) dominates in the overall scattering amplitude. For this purpose we will consider the kinematics close to the condition described in Sec. II.A. Within this kinematics one considers the following ratio:

$$R = \frac{\sigma(Q^2, W, \vec{p}_s)}{\sigma^0(Q^2, W, \vec{p}_s)}, \quad (28)$$

where σ is the differential cross section of eq.(5) that includes both impulse approximation and the rescattering amplitudes, F_a^μ and F_b^μ , respectively. The cross section σ^0 corresponds to the impulse approximation only. Because of the destructive character of the interference between the impulse approximation and rescattering amplitudes above, the ratio has a functional form $R \sim 1 - 2\frac{|F_a F_b|}{|F_a|^2} + \frac{|F_b|^2}{|F_a|^2}$. As follows from eq.(14), the deuteron wave function in F_b^μ enters as $\psi_d(p_s - q)$, compared to $\psi_d(p_s)$ in the impulse approximation of eq.(9). Because of the different arguments appearing in the deuteron wave function, by increasing p_s one should in general expect a more dominant contribution from F_b^μ since it contains the loop integration with effective momenta $|\vec{p}_s - \vec{q}| \leq p_s$.

The analysis of the Ref. [13] demonstrates that the similar ratio for quasielastic $d(e, e'N)N$ scattering exhibits a strong dependence on the spectator nucleon momentum \vec{p}_s . With the increase of p_s , R first decreases below one (because of the dominant contribution from interference term $|F_a F_b|$, usually called the *screening* effect). Then it increases above one as the *double scattering* contribution $|F_b|^2$ becomes dominant.

In Fig. 2 we demonstrate the dependence of R on θ_{sq} , the polar angle of the spectator nucleon with respect to the momentum of the virtual photon. We fix $Q^2 = 1 \text{ GeV}^2$, $W = 1.54 \text{ GeV}$ and chooses two characteristic values for the momenta p_s (200 MeV/c and 400 MeV/c), where, respectively, the screening and double scattering terms are important. Note that the minimum in Fig. 2a and the maximum in Fig. 2b correspond to the value of x and $\frac{E_s - p_{sz}}{m}$ defined by the conditions of eq.(2) and eq.(4), which ensures the maximal contribution from rescattering amplitude F_b^μ (Fig. 1b).

The solid line in Figure 2 corresponds to the calculation within the CQM, where we assume that the hadronic size of the S_{11} is the same as for the nucleon. The dashed line also corresponds to the calculation within the CQM model, but the radius of the S_{11} is described using the relation of eq.(20) with the parameters of the rescattering amplitude defined according to eq.(21). Note that whereas our CQM calculation predicts 15% more screening for the larger S_{11} at $p_s = 200 \text{ MeV/c}$, it reveals more than 50% greater rescattering in the kinematics where double scattering dominates, $p_s = 400 \text{ MeV/c}$. Thus, such an increase of R with the spectator momentum could clearly indicate a large radius of the resonance.

A qualitatively similar picture is obtained for the calculation of R within ECL approach, only now the angular distribution is somewhat broader because of the nondiagonal hadronic state contributions. This is because intermediate states with different mass contribute with different longitudinal momentum transfer due to the term $\sim \frac{m_i^2 - m_j^2}{2p_{fz}}$ in eq.(23) .

A general feature of the R is that at $p_{st} < 300 \text{ MeV}/c$ the screening effects are dominating in eq.(28), thus $R < 1$, and at $p_{st} \geq 300 \text{ MeV}/c$ the dominant character of the double scatterings makes $R > 1$. Such a trend suggests that one can introduce another ratio R_σ , which corresponds to the ratio of the cross section measured say at $p_s \geq 400 \text{ MeV}/c$ to the cross section measured at $p_s \approx 200 \text{ MeV}/c$:

$$R_\sigma(p_{s1}, p_{s2}) = \frac{\sigma(p_s \approx 400 \text{ MeV}/c)}{\sigma(p_s \approx 200 \text{ MeV}/c)}. \quad (29)$$

Because of the different trends of the prediction at the two kinematic ranges, this ratio becomes more sensitive to the hadronic structure of the reinteraction than each cross section does separately.

In Figure 3 we represent the angular dependence of $R_\sigma(p_{s1}, p_{s2})$ normalized by R_{σ_0} calculated for $p_{s1} = 400$ and $p_{s2} = 200 \text{ MeV}/c$. As follows from this figure, the CQM predictions corresponding to the larger resonance radius of eqs.(20) and (21) differ by a factor of 2 from those corresponding to an S_{11} whose radius has been taken equal to the nucleon radius.

Next, we will consider another measurable characteristic which could be complementary to that given above. This is the W dependence (mass distribution) of the cross section at fixed $\frac{E_s - p_{sz}}{m} = 1$ (eq.(4)) and different values of p_{st} .

Within the ECL approach, where the S_{11} represents the superposition of four meson-baryon isospin- $\frac{1}{2}$ states, one expects a larger contribution of the higher-mass intermediate states in the rescattering amplitudes with an increase of W . Specifically, as follows from eq.(23), with an increase of W , the contribution of the more massive $K\Lambda$ and $K\Sigma$ intermediate states will be the least suppressed by the longitudinal momentum. As a result, one may expect that the final state interaction will grow with increase of W .

In Fig. 4 we present the W dependence of the $\sigma_T(d(e, e'\eta p)n)$ cross section calculated according to the eq.(8) within the ECL approach. The cross sections are normalized by the square of the deuteron wave function $|\psi_d(p_s)|^2$ and by values of R calculated at $W = 1.54 \text{ GeV}$. The calculations are done at $Q^2 = 1 \text{ GeV}^2$ for fixed $\frac{E_s - p_{sz}}{m} = 1$ and for different values of p_{st} . The figure shows little deformation of the mass distribution for kinematics where the rescattering results from the screening effect (at $p_{st} \leq 200 \text{ MeV}/c$). This reflects the fact that while the real part of the rescattering amplitude makes the W distribution broader, the increased contribution of the intermediate masses into the imaginary part of the rescattering amplitude results in a sharpening of the W distribution (because of more absorption at $p_{st} \leq 200 \text{ MeV}/c$). Thus these two effects tend to cancel each other, and the resulting distribution is less affected by the final state interaction.

For kinematics where double scattering dominates, both the real and the imaginary parts of the rescattering amplitude work in the same direction, to broaden the W distribution. Here one observes a substantial broadening of the mass distribution. Such a broadening is the essential signature of the composite nature of the resonance.

Figure 5 presents the analogous W dependence of $\sigma_{tot}(d(e, e'\eta p)n) = 4\pi(\sigma_T + \epsilon\sigma_l)$ calculated within the CQM approach. For the calculation of the electromagnetic transition part of the cross section $\gamma^*N \rightarrow N\eta$, we used the parameterization of $\sigma_{tot}(\gamma^*p \rightarrow p\eta)$ from Refs. [27]. As in the case of Figure 4, the calculations were done at $Q^2 = 1 \text{ GeV}^2$ for fixed $\frac{E_s - p_{sz}}{m} = 1$ and different values of p_{st} .

As follows from eq.(15) and eq.(16), the W dependence of the FSI amplitude is mainly due

to the term $\frac{W^2 - m_{N^*}^2}{2p_{fz}}$. Because the kinematics was chosen with $\frac{E_s - p_{sz}}{m} = 1$, such dependence will suppress the FSI amplitude at $W > m_{N^*}$ ($W < m_{N^*}$). Thus one would have less FSI in the tails of the W distribution. Note that because p_{fz} grows with W , some additional W dependence comes from the term $i\Gamma m_R/(2p_{fz})$, which will slightly shift the maximum of the FSI to larger W .

Because of the suppressed FSI in the tails of W distribution, one observes a broadening of the overall W distribution for kinematics where the FSI results from screening ($p_{st} \leq 0.2 \text{ GeV}/c$) compared to the W distribution within the IA. However, for the kinematics of double scattering, $p_{st} \geq 0.3 \text{ GeV}/c$ where the FSI becomes dominant, the W dependence of the FSI has the opposite effect on the overall W dependence of the cross section compared to the IA contribution.

Comparing Figs. 4 and 5, one concludes that the W dependence of the FSI is opposite within the ECL and CQM. Within the ECL, at larger W one has a larger FSI because of the increased contribution of the large mass intermediate states. On the other hand, within the CQM, the FSI is smaller at larger W because of the larger longitudinal momentum transfer entering into the FSI amplitude. Note that this sensitivity of the FSI on W will be suppressed with an increase of Q^2 (p_{fz}). The suppression will be more pronounced within the CQM, since the W dependence is determined mainly by the factor Δ of eq.(16).

IV. FURTHER PROBLEMS THAT CAN BE ADDRESSED

Class of the resonances which can be investigated by similar reactions:

From the discussion of the previous section, we see that the radius of a baryon resonance, which scales sensitively according to the orbital quantum numbers of the quarks in it in a definite model (e.g., that of Ref. [8]), bears a rather straightforward relationship to the quantum numbers of the resonance itself. Since the electro-production of a baryon resonance in the type of experiment we study is sensitive to its mean-square radius, and since there is a rich variety of such baryon resonances with various quantum numbers, the opportunity arises to determine experimentally whether a scaling relationship based on these simple ideas describes the structure of the baryon resonances.

Whereas we have discussed the size determination only in the context of the S_{11} , extending the study to other resonances is straightforward within the same theoretical framework. The extent to which an experimental study would be feasible for other resonances will depend on the rates, which in turn will depend upon the magnitude of the coupling of the photons to the baryon resonances in question, and the size of the theoretical background amplitudes for $NN \rightarrow NN^*$ and charge-exchange amplitudes. An examination of the data on resonance production [16] shows that the same upper limit applies for all other baryon resonances studied as it does to the $S_{11}(1535)$. The nondiagonal transition cross section will be even more suppressed for the higher-mass baryon resonances than it is for the $S_{11}(1435)$ because of the larger value of ΔE discussed in Sect. II.C.

By varying the kinematics (e.g., x according to eq.(2)), we have the possibility of kinematically selecting the baryon resonance whose size we are interested in studying. However, for selecting a given resonance, the kinematics is not the only relevant consideration. Because

there are generally other resonances in the same region of Q^2 and q_0 , additional experimental constraints are desirable. For example, in the case of the $S_{11}(1535)$, the $D_{13}(1520)$ lies nearby in energy. The S_{11} may be separated from this by taking advantage of the fact that the S_{11} has a relatively large branching ratio for η meson decay. Additionally, consideration of the electromagnetic form factor shows that requiring $Q^2 \geq 1\text{GeV}^2$ tends to emphasize the S_{11} over the $D_{13}(1520)$ [2].

Because the D_{13} is favored for the smaller Q^2 values, this resonance may thus be selected by changing Q^2 . Like the S_{11} , the D_{13} is a negative parity resonance and corresponds to a quark excited up by one shell. In the simple quark model, we would therefore expect the spatial distribution of quarks to be similar to that of the S_{11} , and hence the behavior of the reaction cross section $d(e, e'D_{13})n$ should be similar to that of the S_{11} .

The Δ_{33} resonance would be another interesting case, since in the simple quark model all three quarks are in s-wave orbits. Thus, in contrast to the S_{11} , the spatial distribution of the quarks in the Δ_{33} is expected to be more compact. Its reaction $d(e, e'\Delta_{33})n$ should therefore show less pronounced final state interactions than the S_{11} , behaving more similarly to the nucleon. The Δ_{33} should be easy to detect and analyze since it is a strongly excited, isolated resonance.

Another case of interest would be the positive parity $F_{15}(1680)$. In the simple quark model, this resonance involves the promotion of one quark two shells up [8], and thus the increase in the quark spatial distribution would be even more dramatic than in the case of the S_{11} or D_{13} . We find for this resonance that $(\sigma_{hN}^{tot}, b) = (5/3\sigma_{NN}^{tot}, 4/3b_{NN})$. Thus, the interference of the rescattering diagram with the impulse approximation amplitude may have a very pronounced signature. Because of the existence of other resonances in the same energy region (such as the $D_{15}(1675)$), the F_{15} may be more difficult to separate from the background, requiring additional information, perhaps with polarized measurements. However, the F_{15} resonance is known to be strongly excited with increasing Q^2 out to at least 3 GeV^2 [2], so it is an attractive candidate for study using these same theoretical techniques. Finally, it is worth mentioning that in case of the production of states with $L > 0$ and $S > 1/2$, it would be interesting to try to observe spin effects in the rescatterings. In this case, the resonances produced should be polarized due to the FSI, because of the different color separations for states (projections) with different helicities (cf. [28]).

Relations to other nuclear effects:

It is worth noting that the size of resonances as suggested here is an important consideration for the interpretation of other reactions such as electroproduction [29] and pion scattering [30] from nuclei in the GeV range of energies, where resonance excitation is important.

To unambiguously interpret such experiments, one would like to know, say from geometrical considerations, whether the quark distributions of resonances produced in the interior of nuclei significantly overlap those of the nucleons of the nucleus. This has a bearing on whether the resonances can be treated as quasiparticle excitations. The Δ_{33} is an example of a resonance believed to propagate as a quasiparticle, and its medium-modified mass and widths have been determined in this situation from meson factory data [31]. The situation is less clear for higher-mass resonances. However, theoretical analysis of higher energy pion scattering data with such a quasiparticle assumption shows that significant medium effects

occur for the more massive resonances as well [32].

With respect to the quasiparticle assumption, an important property that can be studied in the reactions considered in this paper is the compositeness of the resonance, or in other words the distribution of the constituents that make up the resonant amplitude. Here one expects a sensitivity of the mass distribution of final hadronic states to the contribution of different intermediate states in the scattering processes. Such a sensitivity is substantial at the kinematics dominated by hadronic reinteractions. Note that the qualitative picture one obtains for the deuteron target in rescattering kinematics is similar to the picture of the composite hadronic system in nuclear matter [34,35].

V. SUMMARY

The study of the hadronic properties of baryonic resonances has been carried out theoretically using $d(e, e'R)N$ reactions, where the spectator nucleon N is detected in a special kinematics that allows substantial reinteraction of the electromagnetically produced hadronic system with the spectator nucleon. In particular, the production of the S_{11} resonance in the $d(e, e'S_{11})N$ reaction has been studied.

These reactions were shown to be very sensitive to the hadronic radius of the resonance. Measurements such as the ratio of the cross sections measured at different values of spectator momenta can yield as much as factor 2 difference for the CQM models calculated using different assumptions for the spatial distribution of the quarks in the resonance. In one case we assumed that the size of the resonance was equal to the nucleon size and in another that it scales according to relations suggested by the harmonic oscillator wave function of its constituent quarks.

Next we studied the sensitivity of the $d(e, e'S_{11})N$ reactions to the composite nature of the produced resonance. We applied here the ECL approach to describe the S_{11} as a superposition of multi-channel meson-baryon wave functions with total isospin $\frac{1}{2}$. As compared to the CQM approximation, the ECL approach predicts a qualitatively different picture for the interaction, in that the rescatterings now depend on the relative contribution of the different channels in the intermediate state. In particular, one consequence of the composite nature of the resonance within the ECL approach is a different pattern (in fact, the opposite pattern) of broadening for the mass distribution due to final state interactions.

To summarize, the results of the analysis given here suggests that the electroproduction of baryon resonances on the deuteron can provide a sensitive measure of the hadronic properties of resonances. This can be achieved by using special kinematics where the dominant contribution of the reaction comes from the hadronic reinteraction amplitude. Note that such an experiment might be carried out at TJNAF for the case of the S_{11} resonance, for which the theory and numerical results are worked out in this paper.

ACKNOWLEDGMENTS

Very special thanks are due T. Waas who helped with understanding of the details of the ECL calculations and provided the computation of t -matrices and electromagnetic amplitudes within ECL. Authors also thankful to N. Isgur, V. Burkert, N. Kaiser and G. Piller

for useful discussions. M.Sargsian is grateful to the Alexander von Humboldt foundation for support. This work was supported in part by the German-Israeli Foundation Grant GIF-I-299.095, the U.S. Department of Energy under Contract No. DE-FG02-93ER40771, and the BMBF.

REFERENCES

- [1] V. Burkert, *Leptonic Production of Baryon Resonances* Perspectives in the Structure of Hadronic Systems. Edited by M. N. Harakeh et al., Plenum Press. New York, 1994.
- [2] P. Stoler *Baryon Form Factors at High Q^2 and the transition to perturbative QCD*, Phys. Rep. **226**, 104 (1993).
- [3] M.D. Sokoloff, et al., Phys. Rev. Lett. **57**, 3003 (1986).
- [4] M.R. Adams, et al. Phys. Rev. Lett. **74**, 1525 (1995)
- [5] M. Derrick et al. Phys. Lett. **B356**, 601 (1995); **350**, 120 (1995); T. Ahmed et al., **B338**, 507 (1994);
- [6] R. Weiss-Babai, E971, to be published.
- [7] L.L. Frankfurt, G.A. Miller and M.I. Strikman Ann. Rev. Nucl. Sci. **45**, 501 (1994).
- [8] N. Isgur and G. Karl, Phys. Lett. **B72**, 109 (1977) and Phys. Rev. **D28**, 4187 (1978); N. Isgur and G. Karl, Phys. Rev. **D19**, 2653 (1979).
- [9] W. Konen and H.J. Weber, Phys. Rev. **D41**, 2201 (1990).
- [10] N. Kaiser, P.B. Siegel, W. Weise, Phys. Lett. **B362**, 23 (1995).
- [11] N. Kaiser, T. Waas, W. Weise, Nucl. Phys. **A612**, 297 (1997).
- [12] N. Kaiser, P.B. Siegel, W. Weise, Nucl. Phys. **A594**, 325 (1995).
- [13] L. Frankfurt, G. Miller, W. Greenberg, M. Sargsian, M. Strikman, Z.Phys **A352** 1995; Phys. Lett. **B369**, 201 (1996).
- [14] H. Arenhövel, W. Leidemann, E.L. Tomusiak, Phys. Rev. **C46**, 455 (1992).
- [15] L. Frankfurt, M. Sargsian, M. Strikman, Phys. Rev. **C56** 1124 (1997).
- [16] E. W. Anderson, et al., Phys. Rev. Lett. **16** (1966) 855; R. M. Edelman, et al., Phys. Rev. **D5** (1972) 1073.
- [17] G. Alberi and G. Goggi, Phys. Rev. **74**, 1 (1981).
- [18] J.F. Gunion and Davison E. Soper Phys.Rev. **D15**, 2617 (1977).
- [19] B. Povh and J. Hüfner, Phys. Rev. Lett. **58**, 1612 (1987).
- [20] M. Lutz and W. Weise, Nucl. Phys. **A518**, 156 (1990).
- [21] R. Feynman, *Photon Hadron Interactions*, W.A. Benjamin Inc., 1972.
- [22] V. Franco and R.G. Glauber, Phys. Rev. **142**, 1195 (1966)
- [23] L. Frankfurt, W. Koepf, J. Mützbauer, G. Piller, M. Sargsian and M. Strikman, Nucl. Phys. **A622**, 511 (1997).
- [24] G. E. Brown and A. D. Jackson, *The Nucleon-Nucleon Interaction*, North Holland Publishing Co., 1976.
- [25] L.D. Landau and E. Lifshitz, Oxford ; New York : Pergamon Press, 1977.
- [26] T. Waas, Private communication.
- [27] F.W. Brasse, W. Flauger, et al., Z.Phys **C22**, 33 (1984); J.C.Alder, F.W. Brasse et al.; Nucl. Phys. **91**, 386 (1975).
- [28] L. Gerland, L. Frankfurt, M. Strikman, H. Stöcker and W. Greiner, Phys. Rev. Lett. **81**, 762-765 (1998).
- [29] L. Elouadrhiri et al., Phys. Rev. **C50**, R2266 (1994).
- [30] T. Takahashi et al., Phys. Rev. **C51**, 2542 (1995).
- [31] L. S. Kisslinger and W. Wang, Phys. Rev. Lett. **30**, 1071 (1973); Ann. Phys. (N.Y.) **99**, 374 (1976).
- [32] C. M. Chen, et al., Phys. Rev. **C52**, R485 (1995).
- [33] M. Rößig-Landau et al., Phys. Lett. **B373**, 45 (1996).

- [34] F. Klingl, N. Kaiser, and W. Weise, Nucl. Phys. **A624**, 527 (1997).
- [35] T. Waas and W. Weise, Nucl. Phys. **A625**, 287 (1997).

FIGURES

FIG. 1. Diagrams corresponding to the reaction $e + d \rightarrow e' + N^* + N$. Kinematics have been chosen in a way that suppress the contribution from the N^* component of the deuteron ground state wave function.

FIG. 2. Dependence of R on the angle of the spectator nucleon with respect to transferred momentum q . Solid lines - calculations where rescattering amplitude for S_{11} set as NN amplitude of elastic scattering. Dashed line - $S_{11}N \rightarrow S_{11}N$ amplitude calculated within CQM. Dash-dotted curve corresponds to the calculations within ECL approach, for ηN final state. Curves in (a) correspond to the spectator momenta $p_s = 200 \text{ MeV}/c$ and in (b) $p_s = 400 \text{ MeV}/c$. $W = 1.54 \text{ GeV}$ and $Q^2 = 1 \text{ GeV}^2$.

FIG. 3. Dependence of R_σ (normalized by R_σ calculated within IA) on the angle of the spectator nucleon with respect to transferred momentum q . The kinematics and definition of the curves are the same as in Fig.2.

FIG. 4. Dependence of transverse cross section σ_T of $d(e, e'(\eta N))N$ scattering, on the mass of the produced hadronic state W , calculated within ECL approach. Different curves correspond to different values of spectator nucleon transverse momenta p_{st} at fixed $\frac{E_s - p_{sz}}{m} = 1$. Solid curve corresponds to the $p_{st} = 0$, dashed curve - $p_{st} = 0.2 \text{ GeV}/c$, dotted curve $p_{st} = 0.3 \text{ GeV}/c$ and dash-dotted curve $p_{st} = 400 \text{ MeV}/c$.

FIG. 5. Dependence of total cross section $\sigma_{tot} = 4\pi(\sigma_T + \epsilon\sigma_L)$ of $d(e, e'(\eta p))n$ scattering, on the mass of the produced hadronic state W , calculated within CQM approach. Different curves correspond to different values of spectator nucleon transverse momenta p_{st} at fixed $\frac{E_s - p_{sz}}{m} = 1$. Solid curve corresponds to the $p_{st} = 0$, dashed curve - $p_{st} = 0.2 \text{ GeV}/c$, dotted curve $p_{st} = 0.3 \text{ GeV}/c$ and dash-dotted curve $p_{st} = 400 \text{ MeV}/c$.

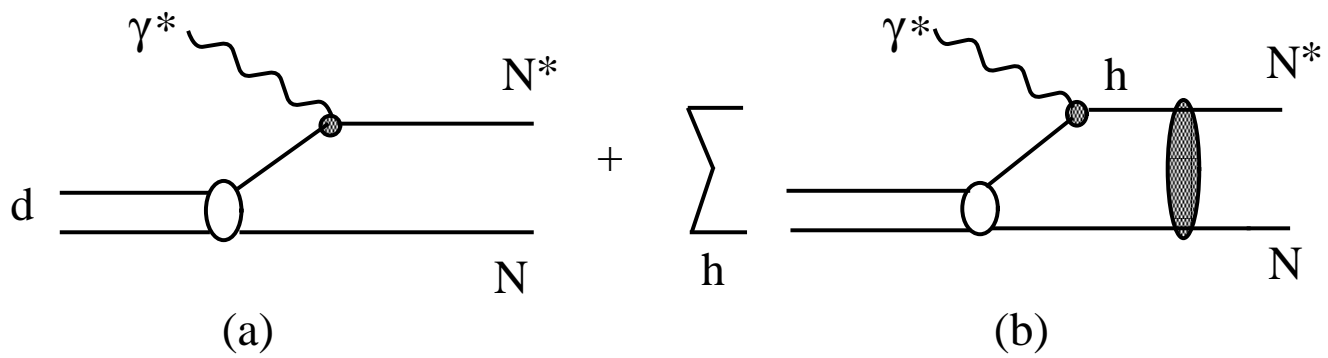


Figure 1

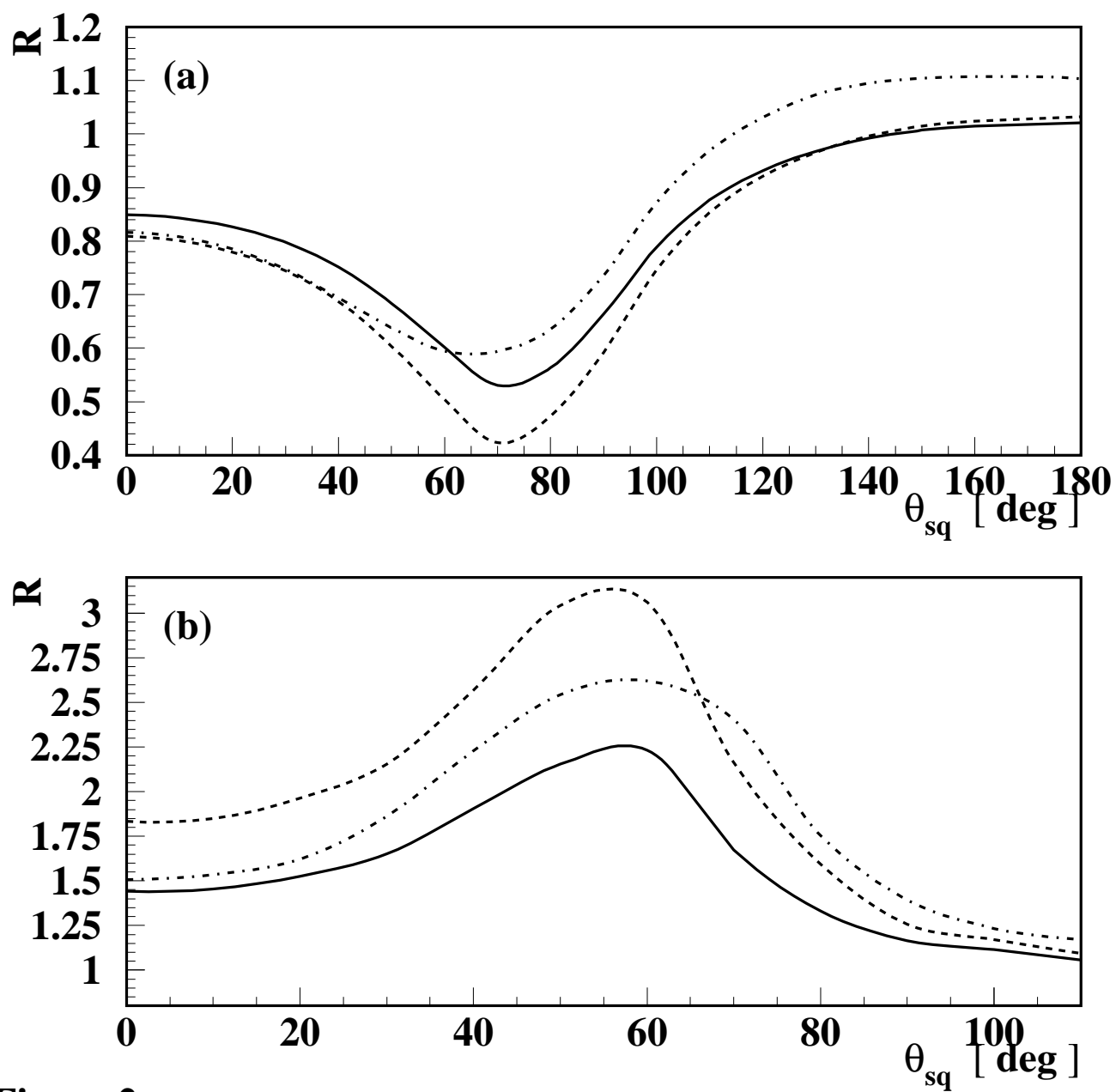


Figure 2

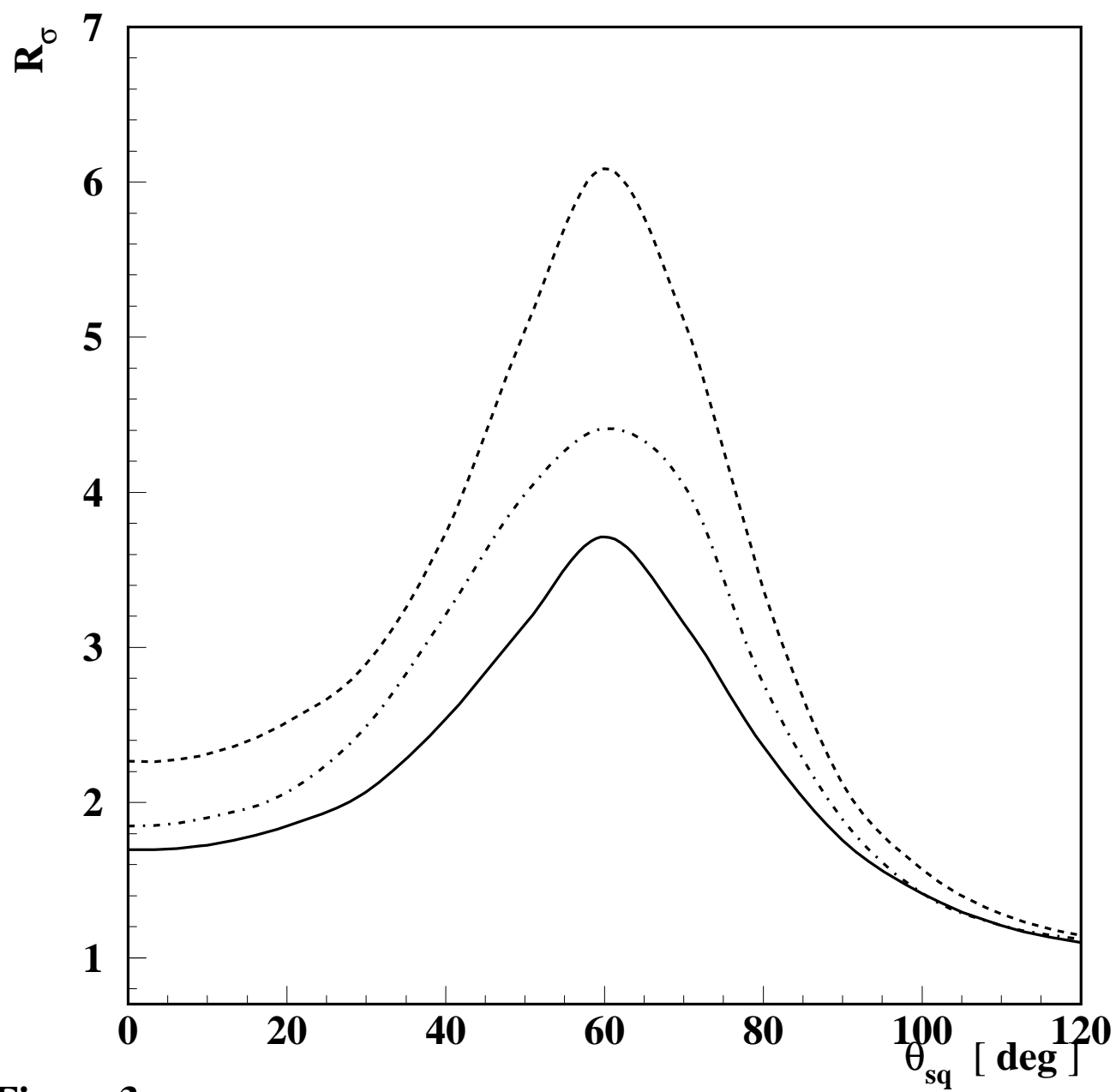


Figure 3

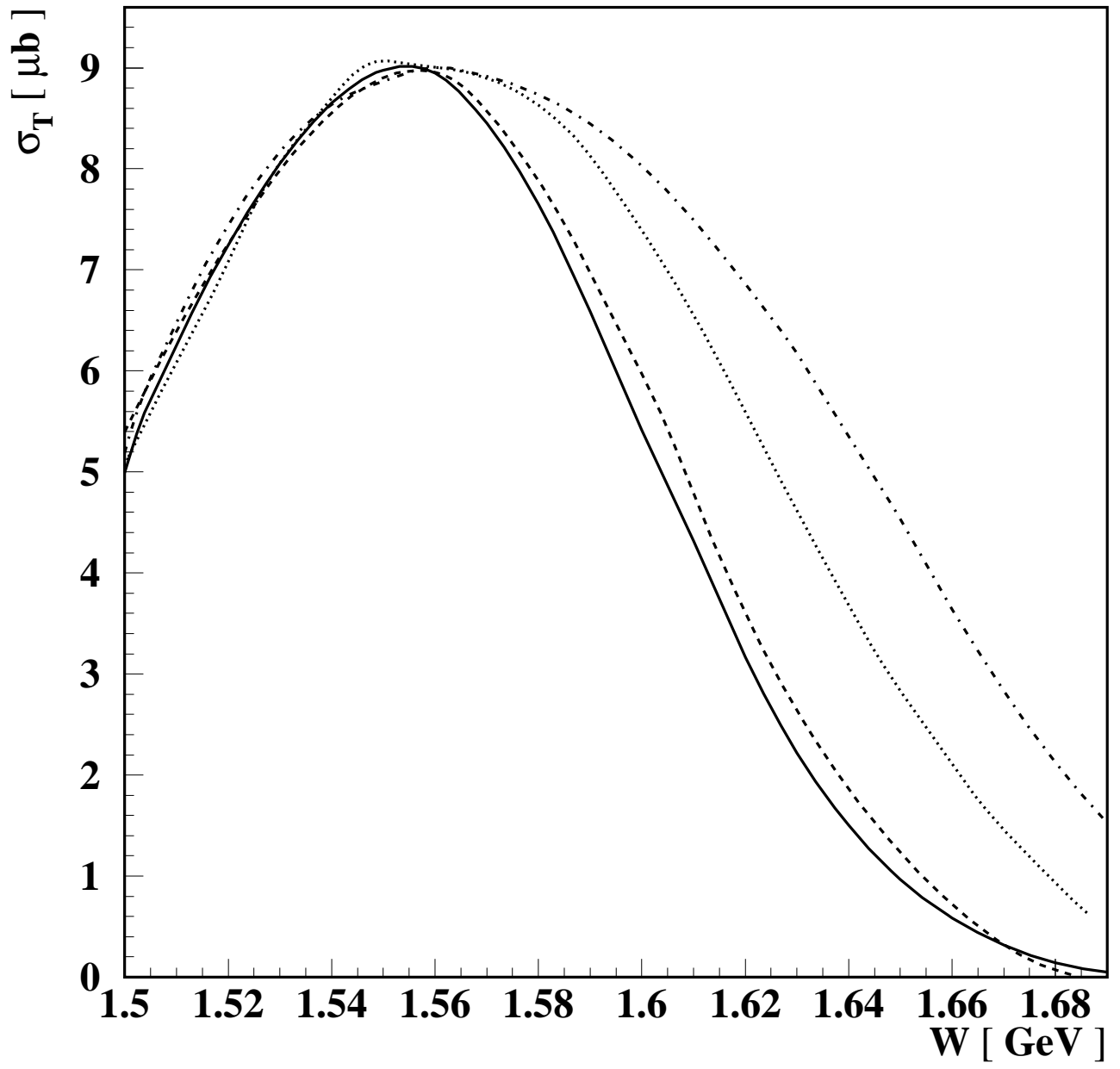


Figure 4

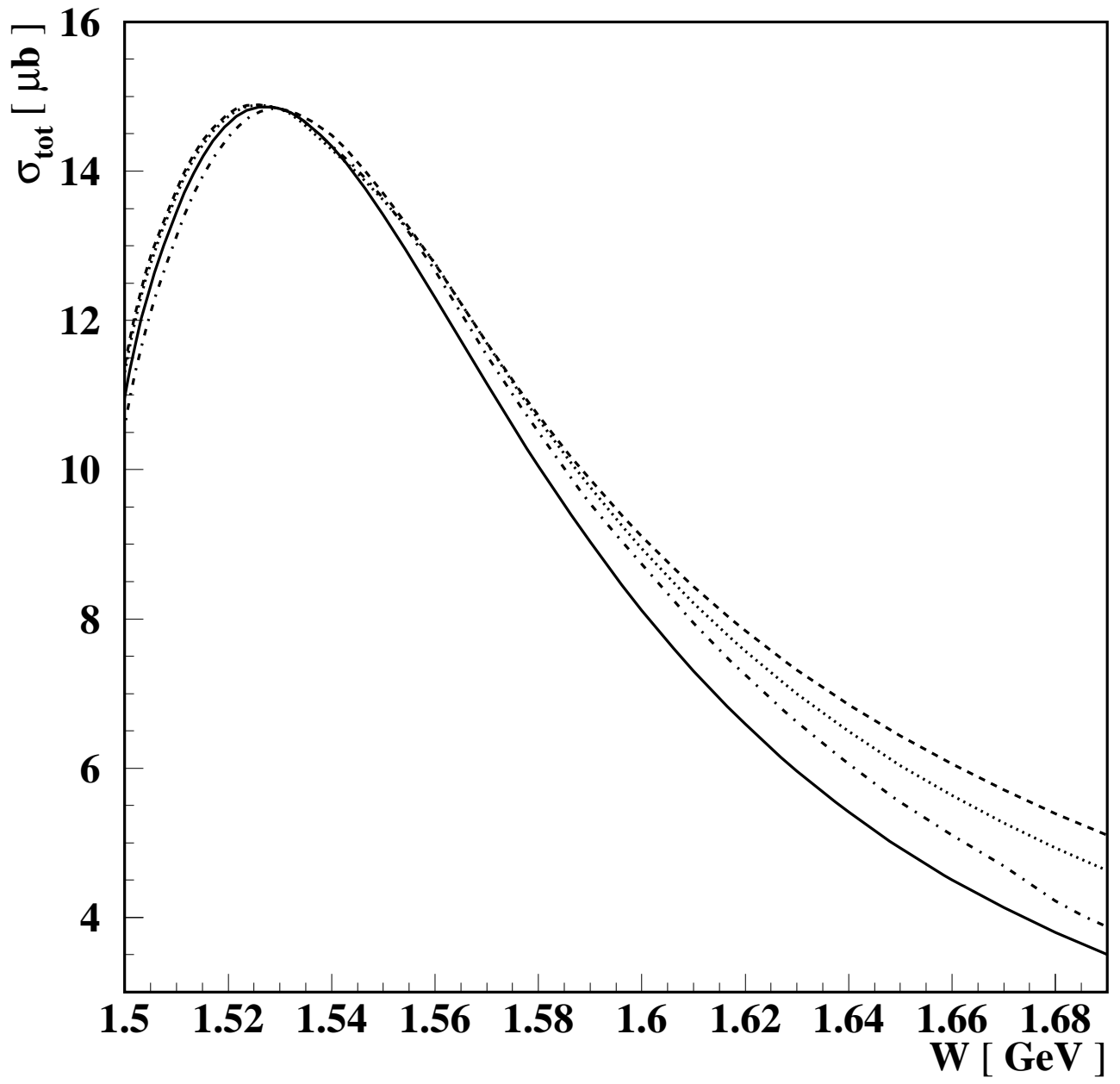


Figure 5